Supporting Information
A Cyclic Triphenylamine Dimer for Organic Field-Effect Transistors with High-Performance

Yabin Song,[†,‡] Chong'an Di,[†,‡] Xiaodi Yang,[†,‡] Shouping Li,[†,‡] Wei Xu,*[,†] Yunqi Liu,*[,†] Lianming Yang,[†] Zhigang Shuai,*[,†] Deqing Zhang,[†] Daoben Zhu*[,†]

Key Laboratory of Organic Solids, Beijing National Laboratory for Molecular Sciences, Institute of Chemistry, Chinese Academy of Sciences, and Graduate School of Chinese Academy of Sciences, Beijing 100080, P. R. China

Complete Ref 3c

3(c) Gelinck, G. H.; Huitema, H. E. A.; van Veenendaal, E.; Cantatore, E.; Schrijnemakers, L.; van der Putten, J. B. P. H.; Geuns, T. C. T.; Beenhakkers, M.; Giesbers, J. B.; Huisman, B.-H.; Meijer, E. J.; Benito, E. M.; Touwslager, F. J.; Marsman, A. W.; van Rens, B. J. E.; de Leeuw, D. M. *Nat. Mater.* 2004, *3*, 106.

Table of contents
1. Synthesis of **1**, **2**.
2. X-ray analysis of **1**.
3. Device fabrication.
4. Theoretical modeling
5. DSC and TGA results of **1**, **2**.
6. UV-Vis spectra of **1**, **2**.
7. Cyclic voltammetry of **1**, **2**.
8. XRD data of **1**, **2**.
9. AFM images of the evaporated films of **1**, **2**.

1. Synthesis of 1, 2.

General. All manipulations of air/moisture-sensitive materials were handled under nitrogen atmosphere using Schlenk techniques. THF were distilled over sodium/benzophenone. Pyridine was distilled over NaOH. All reagents were used as received unless otherwise noted. Melting points were recorded on BÜCHI Melting Point B-500. ^{1}H NMR and ^{13}C NMR spectra were obtained on Bruker Advance 300 or 400 spectrometers. EI-MS measurements were performed on UK GCT-Micromass or SHIMADZU G-MS-QP2010 spectrometers. High-resolution mass spectrometry measurements (HR-MS) were performed on UK GCT-Micromass spectrometers. Elemental analyses were carried out on a Carlo Erba 1106 elemental analyzer.
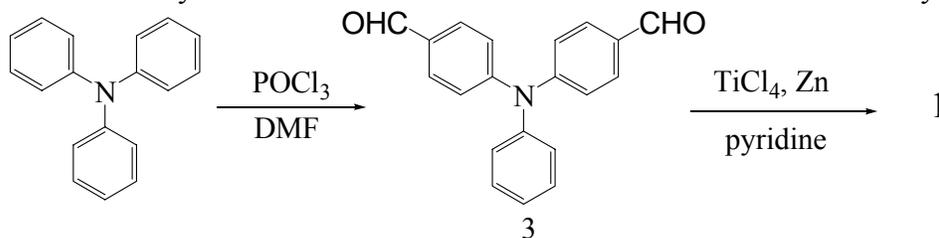
4,4'-diformyltriphenylamine (3). It was prepared from triphenylamine in 65.1% yield

according to the literature procedure[1] with a little modification. ^{1}H NMR (300 MHz, CDCl$_3$) δ 9.90 (s, 2H), 7.80 (d, 4H, J = 8.5 Hz), 7.43 (t, 2H, J = 7.6 Hz), 7.29 (t, 1H, J = 9.0 Hz), 7.20 (d, 4H, J = 8.5 Hz); ^{13}C NMR (100 MHz, CDCl$_3$) δ 190.5, 152.0, 145.5, 131.3, 131.2, 130.2, 127.1, 126.3, 122.8; M. p. 142-143 °C; EI-MS: m/z = 301 (M$^+$); GCT-MS calcd for C$_{20}$H$_{15}$NO$_2$ 301.1103, found 301.1099 (M$^+$).

Compound 1. Zn powder (8.7 g, 132.8 mmol) was suspended in 200 ml THF under N$_2$. A solution of TiCl$_4$ (7.2 ml) in 50 ml CH$_2$Cl$_2$ was added carefully to the suspension with stirring. Then the suspension was refluxing at 80 °C for 1 h. A solution of **3** (1 g, 3.3 mmol) and pyridine (9 ml) in 100 ml THF was added dropwise to the reaction mixture. The mixture was stirred at refluxing for 8 h. After cooling to room temperature, 100 ml saturated aqueous NaHCO$_3$ was added with stirring for 0.5 h. Then it was filtrated, and most of the filtrate was removed under reduced pressure. The residual mixture was extracted twice with dichloromethane (2 × 100 ml), and the combined organic extracts were dried over anhydrous sodium sulfate, filtered, and concentrated in vacuum. The residue was purified by chromatography on silica gel (25% dichloromethane in petroleum ether) to afford 80 mg (9 % yield) of the desired product. Recrystallization from dichloromethane gave rod-like crystals suitable for X-ray crystallographic analysis. M. p. 324-325 °C. ^{1}H NMR (400 MHz, C$_6$D$_6$) δ 6.95-6.88 (m, 8 H), 6.80-6.74 (ABq, 16H, J =8.6 Hz), 6.68 (t, 2H, J = 6.8 Hz), 6.30 (s, 4H); ^{13}C NMR (100 MHz, CDCl$_3$) δ 147.96, 146.58, 132.33, 130.19, 130.03, 128.89, 124.76, 121.50, 121.45; EI-MS: m/z = 538 (M$^+$); HR-MS (GCT-MS): calcd for C$_{40}$H$_{30}$N$_2$ 538.2409, found 538.2412 (M$^+$); Anal. Calcd for C$_{40}$H$_{30}$N$_2$: C, 89.19; H, 5.61; N, 5.20. Found: C, 89.28; H, 5.63; N, 5.30.

(E)-4,4'-bis(diphenylamino)stilbene (2). It was prepared according to literature procedure.[2] ^{1}H NMR (400 MHz C$_6$D$_6$) δ 7.23 (d, 4H, J = 8.4 Hz); 7.14 (s, 4H); 7.12 (s, 4H); 7.09-7.04 (m, 12H); 6.93 (s, 2H); 6.88 (t, 4H, J = 7.2 Hz); ^{13}C NMR (75 MHz CDCl$_3$) δ 147.5, 146.9, 131.8, 129.1, 127.0, 126.2, 124.3, 123.6, 122.8; HR-MS (GCT-MS): calcd for C$_{38}$H$_{30}$N$_2$ 514.2409, found 514.2413 (M$^+$). Anal. Calcd for C$_{38}$H$_{30}$N$_2$: C, 88.68; H, 5.88; N, 5.44. Found: C, 88.74; H, 5.87; N, 5.21.

2. X-ray analysis of 1.

All intensity data were collected with a Bruker SMART CCD diffractometer, using graphite-monochromated Mo KR radiation (λ) 0.71073 Å. The data were collected at 294 K and the structures were resolved by the direct method and refined by full-matrix least-squares on F^2. The computations were performed with the SHELXL-97 program. All non-hydrogen atoms were refined anisotropically. Crystallographic data for **1**: crystal size: 0.22 x 0.20 x 0.16 mm. Triclinic, P-1, Z = 2. a = 10.642(2) Å, b = 10.657(2) Å, c = 13.974(3) Å , α =103.890(3)°, β =105.111(3)°, γ = 90.892(3)°, V =1480.0(5) Å^3, 2θmax = 55.0°, ρ_{calcd} = 1.334 g/cm^3. Of 8320 reflections, 5904 were unique (R_{int} = 0.0160), GOF = 0.999, 379 parameters, $R1$ = 0.0734, $wR2$ = 0.1343 (for all reflections).

3. Device fabrication.

Thin-film transistors were made in a top-contact device configuration. Prior to the deposition, **1** and **2** were purified three times by vacuum sublimation (< 10^{-3} Pa). The substrate was highly n-doped Si with a 450 nm thermally oxidized SiO$_2$ layer on it. Before the deposition of organic semiconductor, octadecyltrichlorosilane (OTS) treatment was performed on the gate dielectrics which were placed in a vacuum oven with OTS at a

temperature of 120°C. Then the treated substrates were rinsed with heptane, ethanol and chloroform, and dried with nitrogen to form OTS self-assembled monolayer on the surface of SiO_2 layer. Thin films of **1** and **2** about 50 nm thick were deposited on Si/SiO_2 at a rate of 1 Å s^{-1}. On top of the thin film's surface, gold was deposited through a shadow mask to give the source (S) and drain (D). The channel length L was 0.05 mm; and the width W was 3 mm. The characteristics of the FETs were obtained at room temperature in air using a Hewlett–Packard (HP) 4140B semiconductor parameter analyzer at different gate voltages.

Theoretical modeling.

We model the charge transport as a Brownian motion process, as described by a particle diffusion process where the mobility can be expressed by the Einstein equation:

$$\mu = \frac{e}{k_B T} D \qquad (1)$$

Where D is the diffusion constant. Taking the crystal structure, we randomly choose one molecule to be the starting point for a particle to diffuse. The hopping is restricted between nearest neighbor molecules. The hopping rate can be described by Marcus theory in the following equation:

$$W = \frac{V^2}{\hbar}\left(\frac{\pi}{\lambda k_B T}\right)^{1/2} \exp(-\frac{\lambda}{4 k_B T}) \qquad (2)$$

Where V is the electronic coupling term and λ is the reorganization energy. The electronic coupling for the hole can be obtained by the direct method:

$$V = < \phi_{HOMO}^{0,site1}\left|F^0\right|\phi_{HOMO}^{0,site2} >=< \phi_{HOMO}^{0,site1}\left|h_{core}\right|\phi_{HOMO}^{0,site2} > + \sum_{l,occ.} <\phi_{HOMO}^{0,site1}\phi_l^0\left|\phi_{HOMO}^{0,site2}\phi_l^0\right. > - < \phi_{HOMO}^{0,site1}\phi_{HOMO}^{0,site2}\left|\phi_l^0\phi_l^0\right. >$$

$$(3)$$

Where the suffix *0* represents the unperturbed monomer, either molecular orbitals or the density matrix. The suffix *site1(2)* represents the molecule 1(2) in the dimer The reorganization energy reflects the geometric changes in the molecules when going from the neutral to the ionized state. We have calculated the reorganization energies at the density functional theory (DFT) level using the B3LYP functional and a 6-31g(d) basis set.

Given the hopping rate between two neighbors, the diffusion coefficient can be evaluated from hopping rate as:

$$D = \frac{1}{2d}\frac{\left\langle x(t)^2 \right\rangle}{t} \approx \frac{1}{2d}\sum_i r_i^2 W_i P_i \qquad (4)$$

i represents a specific hopping path way with r_i being hopping distance (intermolecular center to center distance), and $1/W_i$. being the hopping time. d is the spatial dimension, which is equal to 3 for the crystal. P is the relative probability for a the ith pathway:

$$P_i = W_i / \sum_i W_i \qquad (5)$$

The basic assumption is that the charge transport is a slow process where the solvent and solute molecules have enough time to become equilibrium. This is pertinent for the soft organic system. The drift mobility of hopping, μ, is then evaluated from the Einstein relation. All the quantum chemistry calculations are performed with Gaussian03.[3]

Results:
Part 1: Compound **1**
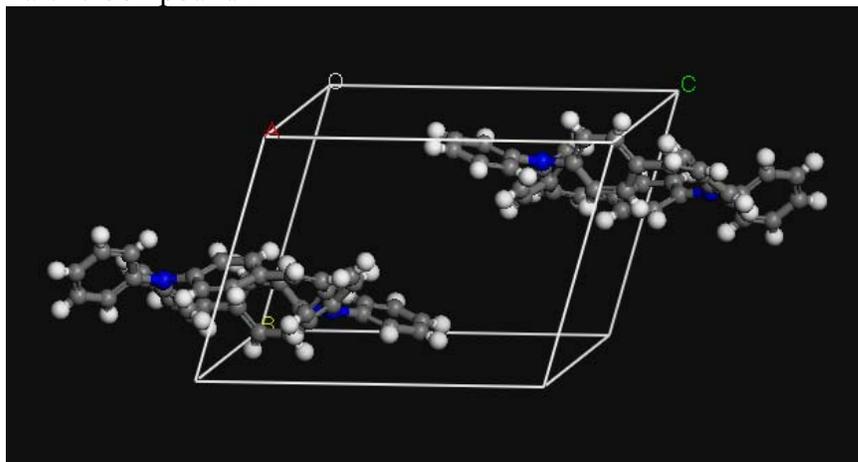
Figure S1. The crystal structure of **1.**
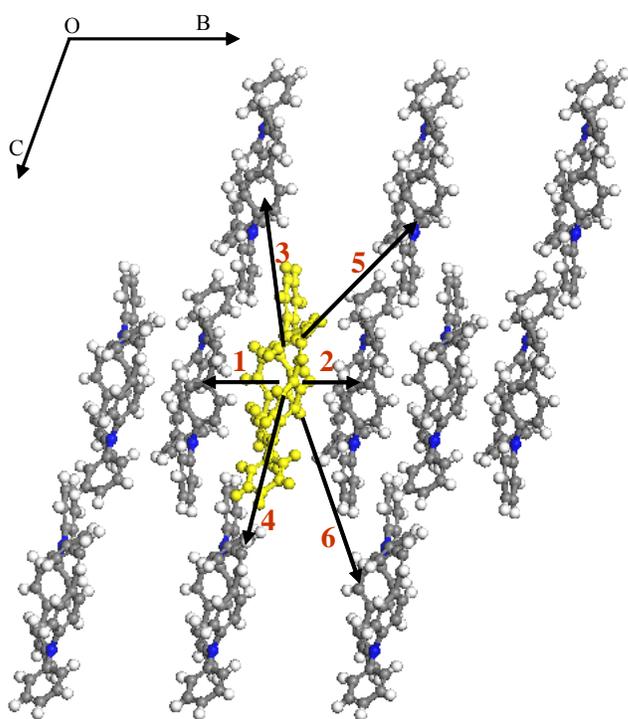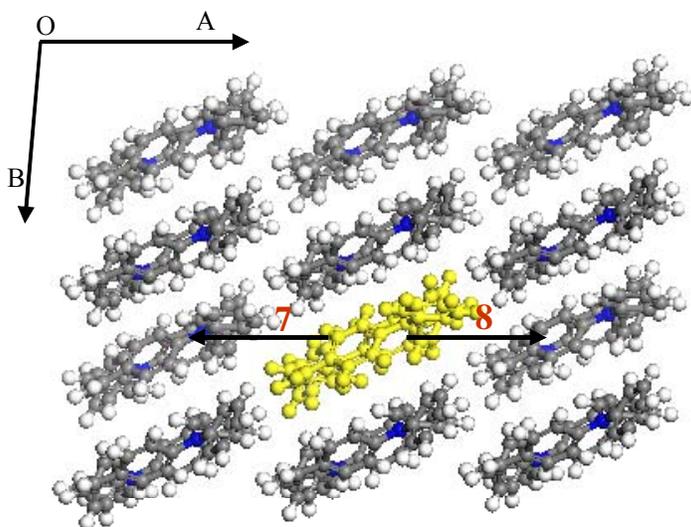
Figure S2. Hoping route of **1** in the crystal.

Reorganization energy is calculated to be 0.1717 eV.

The electronic couplings V for the eight pathways are calculated and given in the following table (DFT/pw91pw91/6-31G*)

pathway	Distance/Å	V (in eV)
1	5.133	4.864E-3
2	5.328	8.652E-3
3	13.502	2.504E-3
4	13.974	7.430E-3
5	15.927	1.356E-7
6	15.406	1.208E-8
7	10.642	4.085E-3
8	10.642	4.092E-3

Drift mobility, μ, cm^2/(V s)　　This work　　2.104×10^{-2}
　　　　　　　　　　　　　　　Experiment　　1.5×10^{-2}

Part 2: linear molecule **2**
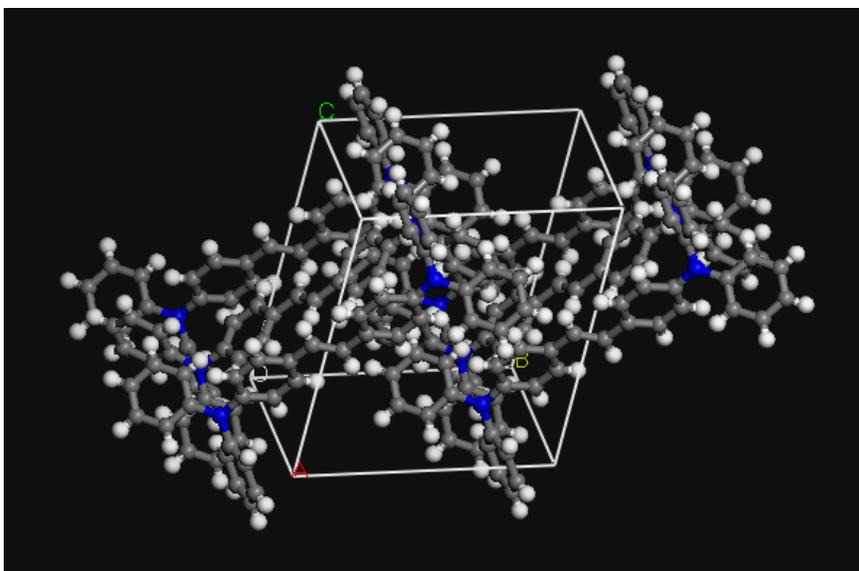
Figure S3. Crystal structure of **2**(according to literature[2]).
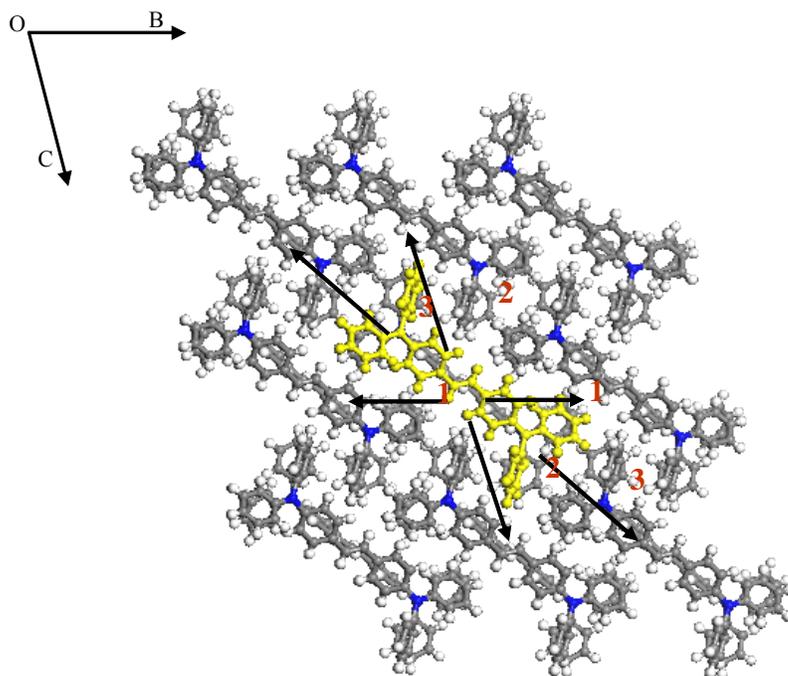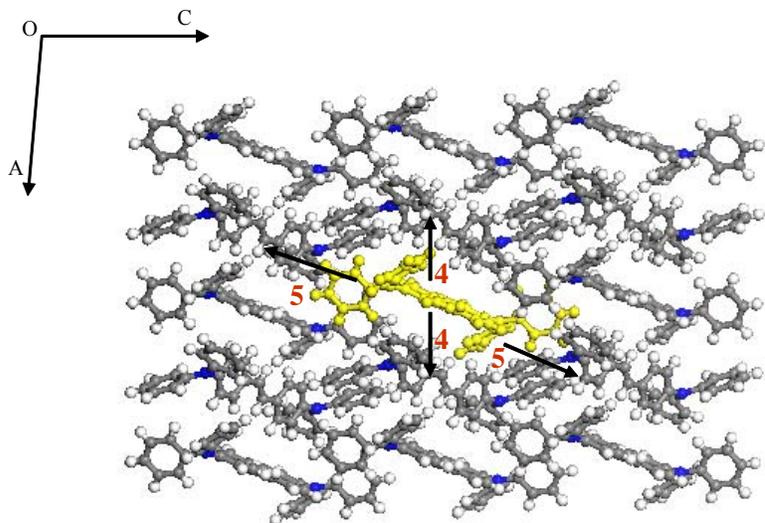
Figure S4. Hoping route of **2** in the crystal.

Compared to **1**, there are two molecules in the 3# lattice. Choose one molecule as the center molecule, we can obtain a drift mobility $\mu=1.31\times10^{-3}$ cm^2/(V s). And get a $\mu=2.58\times10^{-3}$ cm^2/(V s) by choosing the other one. The average value: 1.945×10^{-3}. Reorganization energy is calculated to be 0.3168 eV.

The calculated electronic couplings and mobilities are given in the following table. (DFT/pw91pw91/6-31G*)

dimers	Distance/Å	Electronic coupling/ev
1	11.334	4.348E-3
2	12.491	9.965E-5
3	19.102	2.193E-4
4	5.312	5.644E-3
5	13.575	3.032E-3
Drift mobility, μ, cm^2/(V s)	1.31×10^{-3}	
1	11.334	6.262E-3
2	12.491	1.680E-3
3	19.102	3.081E-3
4	5.312	5.672E-3
5	13.575	3.032E-7
Drift mobility, μ, cm^2/(V s)	2.58×10^{-3}	
The averaged μ, cm^2/(V s)	1.945×10^{-3}	
Experiment	2×10^{-4}	

(a)

(b)
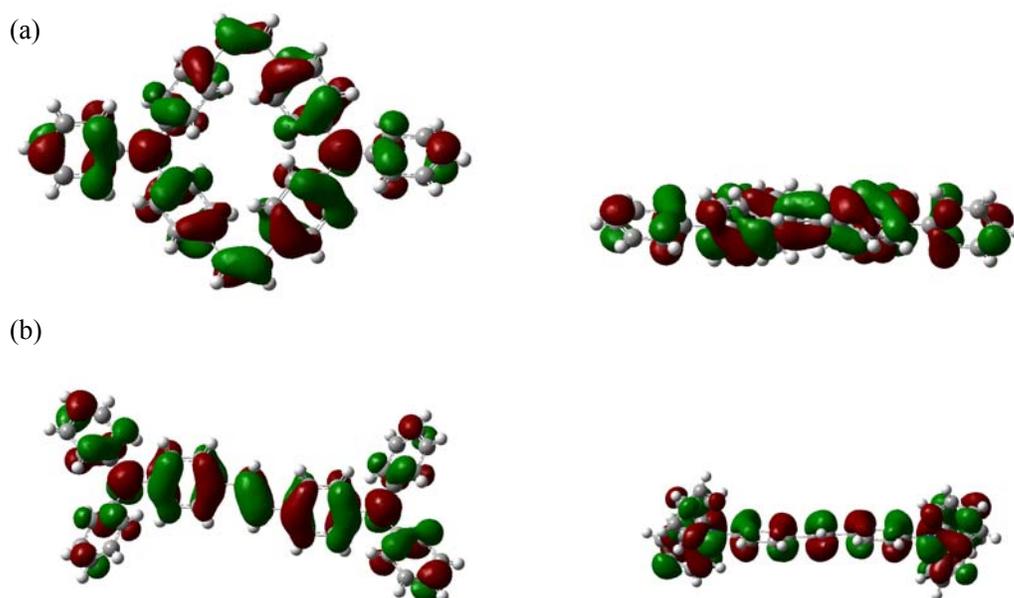
Figure S5. Top view and side view of the molecular HOMO orbital of compound **1 (a)** and **2** (b).

5. DSC and TGA results of 1, 2.

DSC measurements were performed using a Perkin–Elmer differential scanning calorimeter (DSC-7) under N_2 at a heating rate of 10 °C min^{-1}. Thermogravimetric analysis of the molecules was conducted on a TA Instruments SDT2960 TGA. A heating rate of 10 °C min^{-1} under flowing N_2 was used with runs being conducted from room temperature to 800 °C.
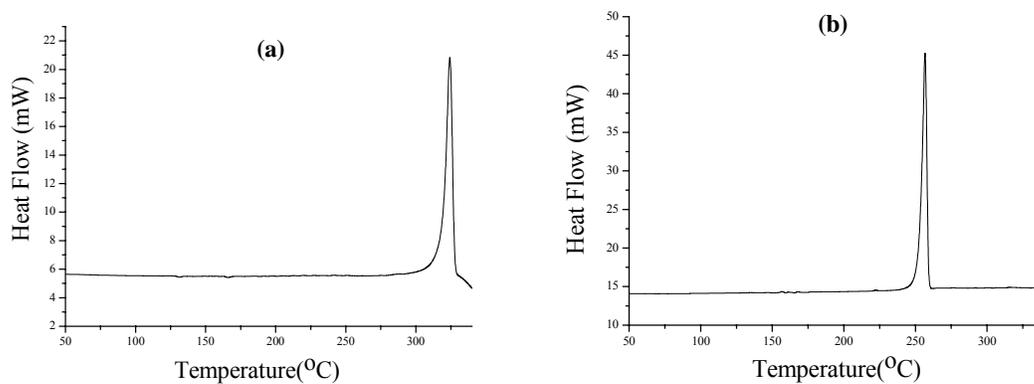
Figure S6. DSC curves of **1** (a) and **2** (b)
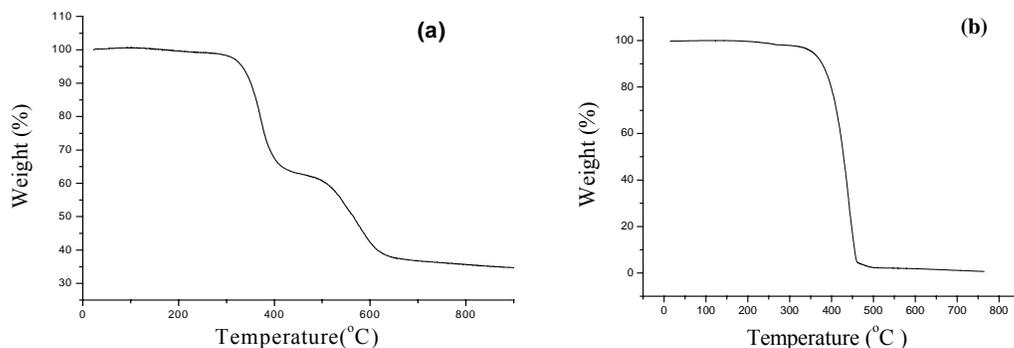
Figure S7. TGA curves of **1** (a) and **2** (b)

6. UV-Vis spectra of 1, 2.

UV-Vis spectra were recorded on a JASCO V-570 spectrometer.
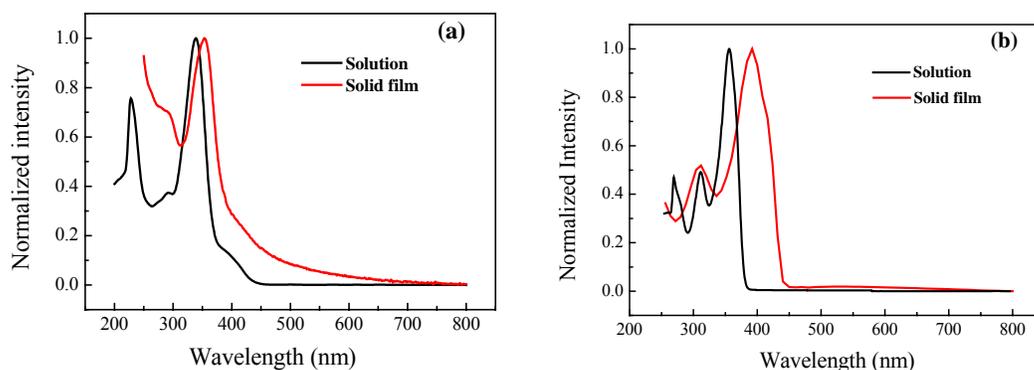
Figure S8. UV-vis absorption spectra of **1** (a) and **2** (b) dilute solutions in dichloromethane and thin films.

7. Cyclic voltammetry of 1, 2.

Cyclic voltammetric measurements were recorded on a CHI660C voltammetric analyzer (CH Instruments, USA). They were carried out in a conventional three-electrode cell using Pt button working electrodes of 2 mm diameter, a platinum wire counter electrode, and a Ag/AgCl reference electrode at room temperature. Conditions: 0.1 M (*n*-Bu)$_4$NPF$_6$ in dichloromethane.
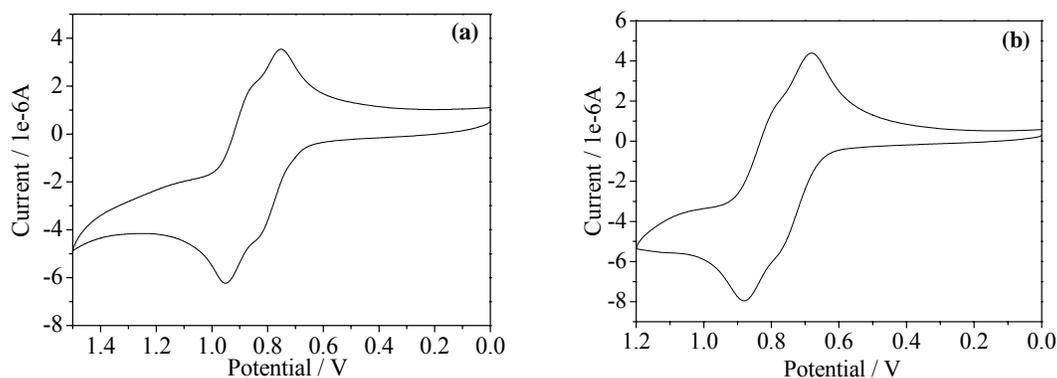
Figure S9. Cyclic voltammograms of **1** (a) and **2** (b).

8. XRD data of 1, 2.

X-Ray diffraction of thin films measurements were performed in reflection mode at 40 kV and 200 mA with Cu Kα radiation using a 2-kW Rigaku X-ray diffractometer.
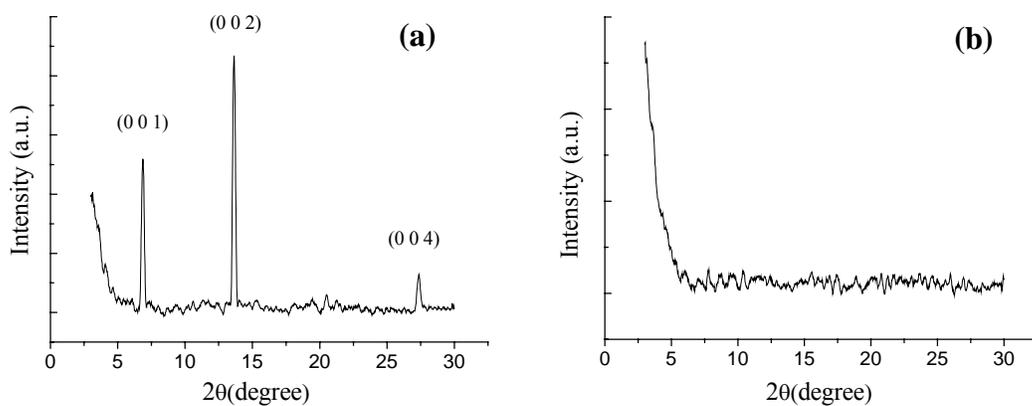
Figure S10. X-ray diffraction patterns of (a) a vacuum-deposited thin film of **1** at 22 ^{o}C. (b) a vacuum-deposited thin film of **2** at 22 ^{o}C.

9. AFM images of the evaporated films of 1, 2.

AFM images of the organic thin films on Si/SiO2 substrate were obtained on a Nanoscope IIIa AFM (Digital Instruments) in tapping mode.
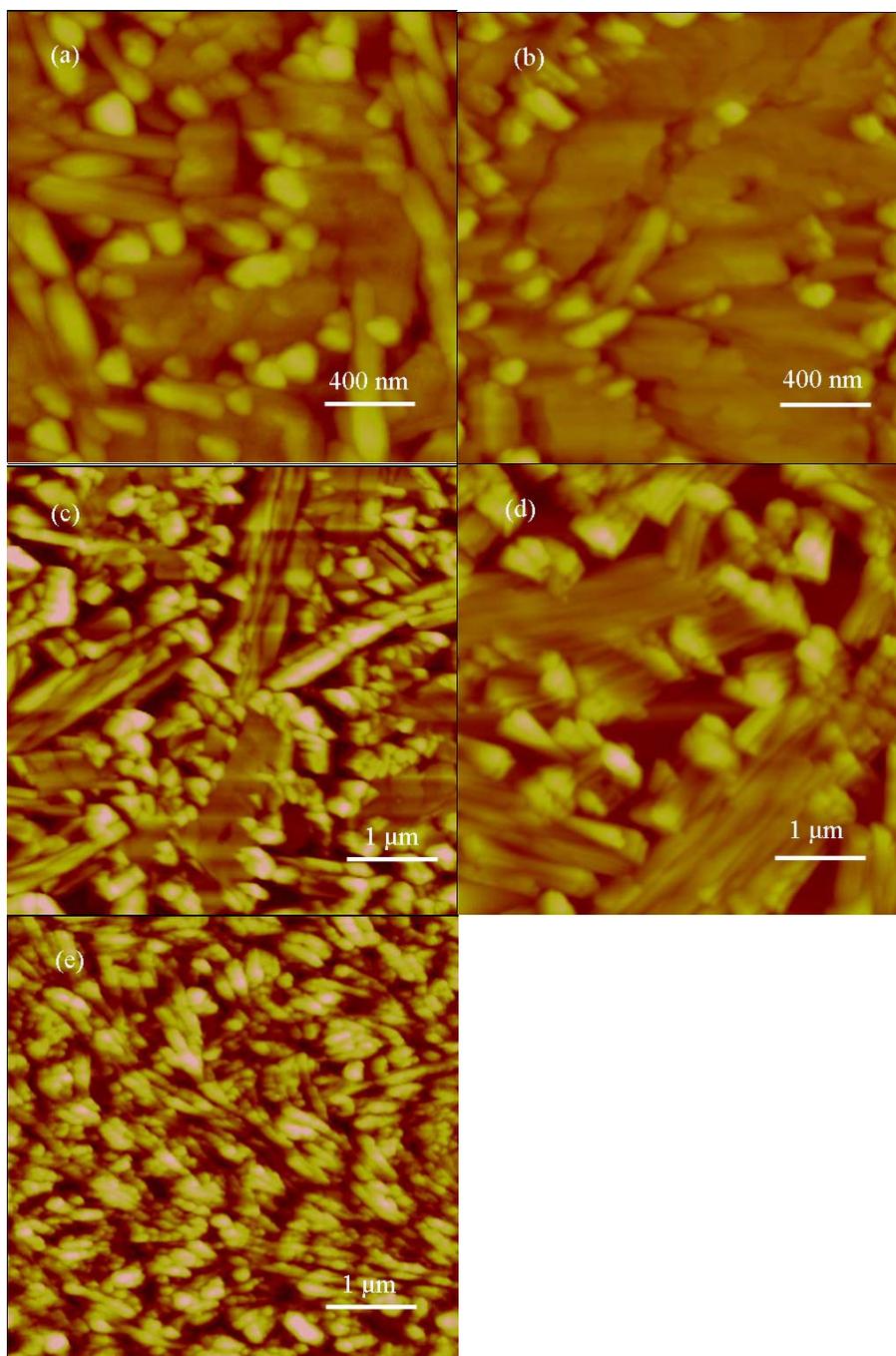
Figure S11. (a) AFM image of **1** on SiO_2 grown at 12 °C. (b) AFM image of **1** at 22 °C. (c) AFM image of **1** at 40 °C. (d) AFM image of **1** at 60 °C. (e) AFM image of **2** at 22 °C.

References
(1) Mallegol, T.; Gmouh, S.; Meziane, M. A. A.; Blanchard-Desce, M.; Mongin; O. *Synthesis* **2005**, *11*, 1771.
(2) Wang, X.; Wang, D.; Zhou, G.; Yu, W.; Zhou, Y.; Fang, Q.; Jiang, M. *J. Mater. Chem.* **2001**, *11*, 1600.

(3) Frisch, M. J.; Trucks, G. W.; Schlegel, H. B.; Scuseria, G. E.; Robb, M. A.; Cheeseman, J. R.; Montgomery, J. A.; Vreven, Jr. T.; Kudin, K. N.; Burant, J. C.; Millam, J. M.; Iyengar, S. S.; Tomasi, J.; Barone, V.; Mennucci, B.; Cossi, M.; Scalmani, G.; Rega, N.; Petersson, G. A.; Nakatsuji, H.; Hada, M.; Ehara, M.; Toyota, K.; Fukuda, R.; Hasegawa, J.; Ishida, M.; Nakajima, T.; Honda, Y.; Kitao, O.; Nakai, H.; Klene, M.; Li, X.; Knox, J. E.; Hratchian, H. P.; Cross, J. B.; Adamo, C.; Jaramillo, J.; Gomperts, R.; Stratmann, R. E.; Yazyev, O.; Austin, A. J.; Cammi, R.; Pomelli, C.; Ochterski, J. W.; Ayala, P. Y.; Morokuma, K.; Voth, G. A.; Salvador, P.; Dannenberg, J. J.; Zakrzewski, V. G.; Dapprich, S.; Daniels, A. D.; Strain, M. C.; Farkas, O.; Malick, D. K.; Rabuck, A. D.; Raghavachari, K.; Foresman, J. B.; Ortiz, J. V.; Cui, Q.; Baboul, A. G.; Clifford, S.; Cioslowski, J.; Stefanov, B. B.; Liu, G.; Liashenko, A.; Piskorz, P.; Komaromi, I.; Martin, R. L.; Fox, D. J.; Keith, T.; Al-Laham, M. A.; Peng, C. Y.; Nanayakkara, A.; Challacombe, M.; Gill, P. M. W.; Johnson, B.; Chen, W.; Wong, M. W.; Gonzalez, C.; and Pople, J. A. Gaussian 03, Revision A.1, Gaussian Inc., Pittsburgh PA, **2003**. The hybrid DFT functional is chosen to be B3LYP, namely, Becke's 3 parameter exchange functional plus Lee-Yang-Parr correlation functional.